X-FEM BASED CONTINUUM SHAPE SENSITIVITY METHOD FOR FRACTURE ANALYSIS OF CRACKS

K Someswara Rao, B N Rao
Department of Civil Engineering, Indian Institute of Technology Madras, Chennai 600 036, INDIA
E-mail of corresponding author: bnrao@iitm.ac.in

ABSTRACT

This paper presents extended finite element method (X-FEM) based continuum shape sensitivity method for calculating the mixed-mode stress-intensity factors of a stationary crack in two-dimensional, linear-elastic, orthotropic materials with arbitrary geometry. The method involves the material derivative concept taken from continuum mechanics, the mutual potential energy release rate, and direct differentiation. The governing variational equation is differentiated prior to discretization. The discrete form of the mutual potential energy release rate is simple and easy to calculate, as it only requires multiplication of displacement vectors and stiffness sensitivity matrices. X-FEM based numerical examples, which comprise mode-I and mixed-mode deformations, are presented to evaluate the accuracy of the fracture parameters calculated by the proposed method. Comparisons have been made between stress-intensity factors predicted by the proposed method and available reference solutions in the literature, generated either analytically or numerically using various other fracture integrals or analyses.

INTRODUCTION

XFEM [1,2] is promising since it avoids using a mesh conforming with the cracks, voids or inhomogeneities, as is the case with the traditional FE method. In XFEM, a standard FE mesh for the problem is first created without accounting for the geometric entity. The presence of cracks, voids or inhomogeneities is then represented independently of the mesh by enriching the standard displacement approximation with additional functions. For crack modelling, both discontinuous displacement fields along the crack faces and the leading singular crack tip asymptotic displacement fields are added to the displacement based FE approximation through the PU method. The additional coefficients at each enriched node are independent. In addition, XFEM provides a seamless means to use higher order elements or special FEs without significant changes in the formulation. XFEM will also improve the accuracy in problems where some aspects of the functional behaviour of the solution field is known a priori and relevant enrichment functions can then be used. As a result, there is considerable interest in developing X-FEM for modelling arbitrary discontinuities in meshes allowing for accurate simulations of crack growth and evolving material interfaces without remeshing and there is need to improve these X-FEM based methods to exploit their potential for practical engineering and industrial applications. In all the aforementioned X-FEM based methods *J*–integral, and/or interaction integral (*M*–integral) is adopted for evaluating the fracture parameters.

Shape sensitivity analysis permits direct, analytical evaluation of first-order (and higher-order, if required) derivatives of potential energy with respect to crack size. Broadly speaking, there are two fundamentally different approaches to shape sensitivity analysis. The first, known as the discrete approach, employs a discretized numerical model (*e.g.*, finite element method [FEM], boundary element method [BEM], mesh-free method, etc.) to approximate the potential energy and then transforms shape derivatives into differentiations of algebraic equations by controlling node motions. The second, known as the continuum approach and adopted in the present work, relies on the variational formulation used in continuum mechanics. In the latter approach, shape sensitivity analysis is conducted by introducing a smooth velocity field to simulate shape change of the initial domain due to the crack advance. While discrete and continuum approaches are related (the former is an approximation of the latter), the continuum approach has two principal advantages: (1) a rigorous mathematical theory is obtained, without the uncertainty/errors associated with finite-dimensional approximation errors; and (2) explicit relations for sensitivity are obtained in terms of physical quantities rather than in terms of sums of derivatives of element matrices. These characteristic features of the continuum approach are of major importance in developing structural optimization theory.

Several shape sensitivity methods involving discrete and continuum formulations have appeared in calculating SIFs. More recently, continuum shape sensitivity methods have also been developed for predicting first-order sensitivities of mixed-mode SIFs for isotropic materials [3-6]. These analytical sensitivities of SIFs provide a convenient means by which subsequent fracture reliability analysis can be performed accurately and efficiently.

However, all of the aforementioned shape sensitivity methods are developed in conjunction with FEM and BEM. There is considerable interest in developing XFEM based shape sensitivity methods for the numerical evaluation of crack-driving forces.

This paper presents extended finite element method (X-FEM) based continuum shape sensitivity method for calculating the mixed-mode stress-intensity factors of a stationary crack in two-dimensional, linear-elastic materials with arbitrary geometry.

BASIC EQUATIONS

Assume there is a discontinuity in an arbitrary domain discretized into some elements with $\boldsymbol{N}$ nodes. In the extended finite element method, the following approximation is utilized to calculate the displacement for point $\boldsymbol{x}$ locating within the domain

$$\boldsymbol{u}^h(\boldsymbol{x}) = \sum_{\substack{I \\ n_I \in N}} \phi_I(\boldsymbol{x})\boldsymbol{u}_I + \sum_{\substack{J \\ n_J \in N^g}} \phi_J(\boldsymbol{x})\psi(\boldsymbol{x})\boldsymbol{a}_J \,, \tag{1}$$

where n_I is the node I, ϕ_I is the shape function associated to node I, $\boldsymbol{u}_I$ is the vector of regular degrees of nodal freedom in finite element method, $\boldsymbol{a}_J$ is the added set of degrees of freedom to the standard finite element model, $\boldsymbol{N}^g$ is the set of nodes that the discontinuity is in its influence (support) domain and $\psi(\boldsymbol{x})$ is the discontinuous function. The influence domain associated to a node, located on an edge, consists of the elements containing that node, whereas for an interior node (in higher order elements) is the element encircling the node. Fig. 1 illustrates the influence domain for a node located on edges of elements.

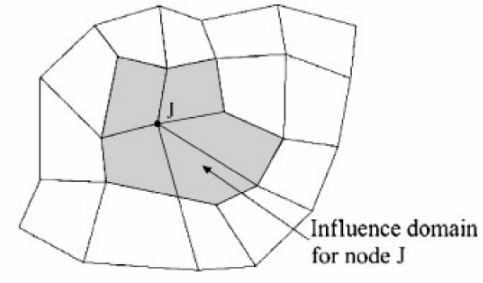

Fig.1: Influence (support) domain for node *J* located on the edge of elements in an arbitrary finite element mesh

The first term in the right-hand side of Eq. (1) is the classical finite element approximation to determine the displacement field, while the second term is the enrichment approximation in order to take into account the existence of any discontinuities. The second term utilizes additional degrees of freedom to facilitate modelling the existence of any discontinuous field, such as a crack, without modelling it explicitly in the finite element mesh.

Modelling crack

Eq. (1) can be re-arranged in order to model crack surfaces and tips in the extended finite element as below

$$\boldsymbol{u}^h(\boldsymbol{x}) = \sum_{\substack{I \\ n_I \in N}} \phi_I(\boldsymbol{x})\boldsymbol{u}_I + \sum_{\substack{J \\ n_J \in N^g}} \boldsymbol{b}_J\phi_J(\boldsymbol{x})H(\boldsymbol{x}) + \sum_{k\in \boldsymbol{K}^1} \phi_k(\boldsymbol{x})\left(\sum_l \boldsymbol{c}_k^{l1}F_l^1(\boldsymbol{x})\right) + \sum_{k\in \boldsymbol{K}^2} \phi_k(\boldsymbol{x})\left(\sum_l \boldsymbol{c}_k^{l2}F_l^2(\boldsymbol{x})\right), \tag{2}$$

where $\boldsymbol{N}^g$ is the set of nodes that have crack face (but not crack-tip) in their support domain, $\boldsymbol{b}_J$ is the vector of additional degrees of nodal freedom and applied in modelling crack faces (not crack-tips), $\boldsymbol{c}_k$ is the vector of additional degrees of nodal freedom for modelling crack-tips, $F_l^i(x)$, $(i=1,2)$, are crack-tip enrichment functions and $\boldsymbol{K}^1$ and $\boldsymbol{K}^2$ are the sets of nodes associated with crack-tip 1 and 2 in their influence domain, respectively. In Eq. (2), $H(\boldsymbol{x})$ is the generalized Heaviside function, simulating the displacement discontinuity in both sides of the crack faces and takes the value $+1$ if $\boldsymbol{x}$ is above the crack and -1, otherwise. If $\boldsymbol{x}^*$ is the nearest point on the crack to $\boldsymbol{x}$ (see Fig. 2) and $\boldsymbol{e}_n$ is the unit vector normal to the crack alignment in which $\boldsymbol{e}_s \times \boldsymbol{e}_n = \boldsymbol{e}_z$ ($\boldsymbol{e}_s$ is the unit tangential vector and $\boldsymbol{e}_z$ is the outward normal to the surface), then

$$H(\boldsymbol{x})=\begin{cases}+1 & \text{if } (\boldsymbol{x}-\boldsymbol{x}^*).\boldsymbol{e}_n>0\\ -1 & \text{otherwise}\end{cases}. \tag{3}$$

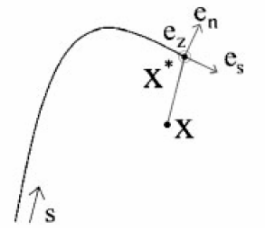

Fig.3: Node selection for enrichment; nodes marked by triangles are enriched by crack-tip functions and the circled ones are enriched by the Heaviside function

Crack-tip enrichment functions for orthotropic linear-elastic media

In LEFM, the asymptotic near tip displacement field $\boldsymbol{u}=\{u_1,u_2\}^T$ for orthotropic materials is given by

$$\begin{aligned}u_1 = {} & K_I\sqrt{\frac{2r}{\pi}}\,\mathrm{Re}\left[\frac{1}{\mu_1-\mu_2}\left\{\mu_1 p_2\sqrt{\cos\theta+\mu_2\sin\theta}-\mu_2 p_1\sqrt{\cos\theta+\mu_1\sin\theta}\right\}\right]+\\ & K_{II}\sqrt{\frac{2r}{\pi}}\,\mathrm{Re}\left[\frac{1}{\mu_1-\mu_2}\left\{p_2\sqrt{\cos\theta+\mu_2\sin\theta}-p_1\sqrt{\cos\theta+\mu_1\sin\theta}\right\}\right]\end{aligned}, \tag{4}$$

$$\begin{aligned}u_2 = {} & K_I\sqrt{\frac{2r}{\pi}}\,\mathrm{Re}\left[\frac{1}{\mu_1-\mu_2}\left\{\mu_1 q_2\sqrt{\cos\theta+\mu_2\sin\theta}-\mu_2 q_1\sqrt{\cos\theta+\mu_1\sin\theta}\right\}\right]+\\ & K_{II}\sqrt{\frac{2r}{\pi}}\,\mathrm{Re}\left[\frac{1}{\mu_1-\mu_2}\left\{q_2\sqrt{\cos\theta+\mu_2\sin\theta}-q_1\sqrt{\cos\theta+\mu_1\sin\theta}\right\}\right]\end{aligned}, \tag{5}$$

where Re denotes the real part of the statement and K_I and K_{II} are stress intensity factors (SIFs) for mode I and mode II, respectively. p_k and q_k are defined as

$$p_k=a_{11}\mu_k^2+a_{12}-a_{16}\mu_k,\quad q_k=a_{12}\mu_k+\frac{a_{22}}{\mu_k}-a_{26}, \tag{6}$$

where

$$\begin{aligned}&a_{\alpha\beta}=s_{ijkl} && \text{if } \alpha,\beta\le 3\\ &a_{\alpha\beta}=2s_{ijkl} && \text{if either } \alpha \text{ or } \beta\le 3,\\ &a_{\alpha\beta}=4s_{ijkl} && \text{if } \alpha,\beta>3\end{aligned}\quad \alpha=\begin{cases} i & \text{if } i=j\\ 9-i-j & \text{if } i\ne j\end{cases},\quad \beta=\begin{cases} k & \text{if } k=l\\ 9-k-l & \text{if } k\ne l\end{cases}, \tag{7}$$

with s_{ijkl} being fourth-order compliance tensor, and μ_1, $\bar{\mu}_1$ and μ_2, $\bar{\mu}_2$ occur in conjugate pairs which are the roots of

$$a_{11}\mu^4-2a_{16}\mu^3+(2a_{12}+a_{66})\mu^2-2a_{26}\mu+a_{22}=0. \tag{8}$$

With the purpose of extracting the crack-tip functions, Eqs. (4) and (5) are transformed into a simpler and practical form. Two auxiliary complex variables, which are the square of main fields in Equations Eqs. (4) and (5), are introduced in polar forms

$$Z_k^{aux}=r_k e^{i\theta_k}=r(\cos\theta+\mu_k\sin\theta), \tag{9}$$

with

$$r_k=rg_k(\theta),\quad g_k(\theta)=\sqrt{(\cos\theta+\mu_{kx}\sin\theta)^2+(\mu_{ky}\sin\theta)^2},\quad \theta_k=\arctan\left(\frac{\mu_{ky}\sin\theta}{\cos\theta+\mu_{kx}\sin\theta}\right). \tag{10}$$

Thereafter, one can rewrite the imaginary and real parts of the main field of Eqs. (4) and (5), $\sqrt{\cos\theta+\mu_k\sin\theta}$, $(k=1,2)$,as

$$\mathrm{Im}\left(\sqrt{Z_k^{aux}}\right)=r^{1/2}\sqrt{g_k(\theta)}\sin\frac{\theta_k}{2},\quad (k=1,2),\quad \mathrm{Re}\left(\sqrt{Z_k^{aux}}\right)=r^{1/2}\sqrt{g_k(\theta)}\cos\frac{\theta_k}{2},\quad (k=1,2), \tag{11}$$

Crack-tip enrichment functions are obtained using Equations Eqs. (4), (5), (10) and (11) as

$$\left\{F_l(r,\theta)\right\}_{l=1}^{4} = \left\{\sqrt{r}\cos\frac{\theta_1}{2}\sqrt{g_1(\theta)}, \sqrt{r}\cos\frac{\theta_2}{2}\sqrt{g_2(\theta)}, \sqrt{r}\sin\frac{\theta_1}{2}\sqrt{g_1(\theta)}, \sqrt{r}\sin\frac{\theta_2}{2}\sqrt{g_2(\theta)}\right\}. \tag{12}$$

SHAPE SENSITIVITY ANALYSIS

Velocity Field

Consider a general three-dimensional body with a specific configuration, referred to as the initial (reference) configuration, with domain Ω, boundary Γ, and a body material point identified by position vector $\boldsymbol{x} \in \Omega$. Consider the body's motion from an initial configuration with domain Ω and boundary Γ into a perturbed configuration with domain Ω_τ and boundary Γ_τ,. This process can be expressed as

$$\boldsymbol{T}:\boldsymbol{x} \to \boldsymbol{x}_\tau, \quad \boldsymbol{x} \in \Omega, \tag{13}$$

where $\boldsymbol{x}_\tau$ is the position vector of the material point in the perturbed configuration, $\boldsymbol{T}$ is a transformation mapping, and $\tau \in \mathbb{R}^+$ is a scalar, fictitious, time-like parameter denoting the amount of shape change, with

$$\begin{aligned} \boldsymbol{x}_\tau &= \boldsymbol{T}(\boldsymbol{x},\tau) \\ \Omega_\tau &= \boldsymbol{T}(\Omega,\tau). \\ \Gamma_\tau &= \boldsymbol{T}(\Gamma,\tau) \end{aligned} \tag{14}$$

A velocity field can then be defined as

$$\boldsymbol{v}(\boldsymbol{x}_\tau,\tau) \equiv \frac{d\boldsymbol{x}_\tau}{d\tau} = \frac{d\boldsymbol{T}(\boldsymbol{x},\tau)}{d\tau} = \frac{\partial \boldsymbol{T}(\boldsymbol{x},\tau)}{\partial\tau}. \tag{15}$$

In the neighborhood of the initial time τ = 0, assuming a regularity hypothesis and ignoring high-order terms,

$$\boldsymbol{x}_\tau = \boldsymbol{T}(\boldsymbol{x},\tau) = \boldsymbol{T}(\boldsymbol{x},0) + \tau\frac{\partial \boldsymbol{T}(\boldsymbol{x},0)}{\partial\tau} + O(\tau^2) \cong \boldsymbol{x} + \tau\boldsymbol{v}(\boldsymbol{x},0), \tag{16}$$

where $\boldsymbol{x} = \boldsymbol{T}(\boldsymbol{x},0)$. For the rest of this paper, the velocity field $\boldsymbol{v}(\boldsymbol{x},0)$ will be denoted by $\boldsymbol{V}(\boldsymbol{x})$ or $\boldsymbol{V}$. Thus, a velocity field characterizes the direction of domain variation, which implies that for a given $\boldsymbol{V}(\boldsymbol{x})$, the shape change of Ω is uniquely controlled by the scalar parameter τ.

Sensitivity Analysis

The variational governing equation for a linear-elastic, solid with domain Ω can be formulated as

$$a_\Omega(\boldsymbol{z},\bar{\boldsymbol{z}}) = \ell_\Omega(\bar{\boldsymbol{z}}), \quad \text{for all } \bar{\boldsymbol{z}} \in \boldsymbol{Z}, \tag{17}$$

where $\boldsymbol{z}$ and $\bar{\boldsymbol{z}}$ are the actual and virtual displacement fields of the structure, respectively, $\boldsymbol{Z}$ is the space of kinematically admissible virtual displacements, and $a_\Omega(\boldsymbol{z},\bar{\boldsymbol{z}})$ and $\ell_\Omega(\bar{\boldsymbol{z}})$ are energy bilinear and load linear forms, respectively. The subscript Ω in Eq. (17) is used to indicate the dependency of the governing equation on the shape of the structural domain. If $\boldsymbol{z}_\tau(\boldsymbol{x}_\tau)$ represents the displacement at $\boldsymbol{x}_\tau = \boldsymbol{x} + \tau\boldsymbol{V}(\boldsymbol{x})$ of the perturbed domain, the pointwise material derivative at $\boldsymbol{x} \in \Omega$ is defined as

$$\dot{\boldsymbol{z}}(\boldsymbol{x}) \equiv \lim_{\tau\to 0}\left[\frac{\boldsymbol{z}_\tau(\boldsymbol{x}+\tau\boldsymbol{V}(\boldsymbol{x})) - \boldsymbol{z}(\boldsymbol{x})}{\tau}\right] = \boldsymbol{z}'(\boldsymbol{x}) + \boldsymbol{\nabla}\boldsymbol{z}^T\boldsymbol{V}(\boldsymbol{x}), \tag{18}$$

where

$$\boldsymbol{z}' = \lim_{\tau\to 0}\left[\frac{\boldsymbol{z}_\tau(\boldsymbol{x}) - \boldsymbol{z}(\boldsymbol{x})}{\tau}\right], \tag{19}$$

is the partial derivative of $\boldsymbol{z}$ and $\boldsymbol{\nabla} = \{\partial/\partial x_1, \partial/\partial x_2, \partial/\partial x_3\}^T$ is the vector of gradient operators.

If no body forces are involved, the variational equation (Eq. (17)) can be written as

$$a_\Omega(\boldsymbol{z},\bar{\boldsymbol{z}}) \equiv \int_\Omega \sigma_{ij}(\boldsymbol{z})\varepsilon_{ij}(\bar{\boldsymbol{z}})d\Omega \;\; = \ell_\Omega(\bar{\boldsymbol{z}}) \equiv \int_\Gamma T_i\bar{z}_i d\Gamma \quad , \tag{20}$$

where $\sigma_{ij}(\boldsymbol{z})$ and $\varepsilon_{ij}(\bar{\boldsymbol{z}})$ are components of the stress and strain tensors of the displacement $\boldsymbol{z}$ and virtual displacement $\bar{\boldsymbol{z}}$, respectively, T_i is the *i*th component of the surface traction, and $\bar{z}_i$ is the *i*th component of $\bar{\boldsymbol{z}}$. Taking the material derivative of both sides of Eq. (20), it can be shown that

$$a_\Omega(\dot{\boldsymbol{z}},\bar{\boldsymbol{z}}) = \ell'_V(\bar{\boldsymbol{z}}) - a'_V(\boldsymbol{z},\bar{\boldsymbol{z}}), \;\; \forall\, \bar{\boldsymbol{z}} \in \boldsymbol{Z}, \tag{21}$$

where the subscript $\boldsymbol{V}$ indicates the dependency of the terms on the velocity field. The terms $\ell'_V(\bar{\boldsymbol{z}})$ and $a'_V(\boldsymbol{z},\bar{\boldsymbol{z}})$

can be further derived as

$$\ell'_V(\bar{\boldsymbol{z}}) = \int_\Gamma \left\{ -T_i(\bar{z}_{i,j}V_j) + \left[(T_i\bar{z}_i)_{,j}\, n_j + \kappa_\Gamma (T_i\bar{z}_i) \right](V_i n_i) \right\} d\Gamma \quad , \tag{22}$$

and

$$a'_V(\boldsymbol{z},\bar{\boldsymbol{z}}) \;=\; -\int_\Omega \begin{bmatrix} \varepsilon_{ij}(\boldsymbol{z}) D_{ijkl}(\boldsymbol{x}) (\bar{z}_{k,m} V_{m,l}) + \varepsilon_{ij}(\bar{\boldsymbol{z}}) D_{ijkl}(\boldsymbol{x}) (z_{k,m} V_{m,l}) - \\ \varepsilon_{ij}(\boldsymbol{z}) D_{ijkl}(\boldsymbol{x}) \varepsilon_{kl}(\bar{\boldsymbol{z}}) \mathrm{div}\boldsymbol{V} \end{bmatrix} d\Omega \,, \tag{23}$$

where n_i is the ith component of unit normal vector $\boldsymbol{n}$, κ_Γ is the curvature of the boundary, $z_{i,j} = \partial z_i / \partial x_j$, $\bar{z}_{i,j} = \partial \bar{z}_i / \partial x_j$, $V_{i,j} = \partial V_i / \partial x_j$, $D_{ijkl}(\boldsymbol{x})$ is a component of the constitutive tensor.

SHAPE SENSITIVITY METHOD FOR FRACTURE ANALYSIS

Consider an arbitrary, two-dimensional cracked body of crack length a, with unit thickness subjected to an arbitrary loading. The total potential energy Π of the system in the absence of body forces is

$$\Pi \equiv \frac{1}{2}\int_\Omega \varepsilon_{ij}(\boldsymbol{z}) D_{ijkl} \varepsilon_{kl}(\boldsymbol{z}) d\Omega \;\; - \int_\Gamma T_i z_i d\Gamma \quad , \tag{24}$$

where, for two-dimensional linear elastic material models, D_{ijkl}, are the components of the constant elasticity matrix

$$\boldsymbol{D} = \begin{cases} \dfrac{E}{1-\nu^2}\begin{bmatrix} 1 & \nu & 0 \\ \nu & 1 & 0 \\ 0 & 0 & \dfrac{1-\nu}{2} \end{bmatrix}, & \text{for plane stress} \\ \dfrac{E}{[1+\nu][1-2\nu]}\begin{bmatrix} 1-\nu & \nu & 0 \\ \nu & 1-\nu & 0 \\ 0 & 0 & \dfrac{1-2\nu}{2} \end{bmatrix}, & \text{for plane strain} \end{cases} . \tag{25}$$

By substituting $\bar{\boldsymbol{z}}$ with $\boldsymbol{z}$ in Eq. (20) and by using Eq. (24), the following is produced

$$\Pi = -\frac{1}{2} a_\Omega(\boldsymbol{z},\boldsymbol{z}) \,. \tag{26}$$

The energy release rate is equal to the derivative of potential energy with respect to the crack area. For a two-dimensional cracked structure with unit thickness, the crack area is equal to crack length a. Assuming crack length a to be the variable of interest, a change in crack area or crack length involves a change in the shape of the cracked continuum. In relation to shape sensitivity theory, such a change implies that the energy release rate is equal to the material derivative of potential energy. Hence, for elastic (linear or nonlinear) solids under mixed-mode loading conditions, the J-integral, which is equal to the energy release rate, can be derived as

$$J \equiv -\dot{\Pi} = \frac{1}{2}\left[a_\Omega(\dot{\boldsymbol{z}},\boldsymbol{z}) + a_\Omega(\boldsymbol{z},\dot{\boldsymbol{z}}) + a'_V(\boldsymbol{z},\boldsymbol{z}) \right], \tag{27}$$

where the overdot indicates a material derivative. If (1) velocity field $\boldsymbol{V}(\boldsymbol{x})$ is defined such that traction-loading boundary Γ is fixed, *i.e.*, $\boldsymbol{V}(\boldsymbol{x}) = \boldsymbol{0}$ on the traction-loading boundary Γ; and (2) $\bar{\boldsymbol{z}}$ is replaced with $\boldsymbol{z}$ in Eq. (21), noting that $a_\Omega(\dot{\boldsymbol{z}},\boldsymbol{z}) = a_\Omega(\boldsymbol{z},\dot{\boldsymbol{z}}) = -a'_V(\boldsymbol{z},\boldsymbol{z})$, then

$$J = -\frac{1}{2} a'_V(\boldsymbol{z},\boldsymbol{z}) \,. \tag{28}$$

Substituting the expression of $a'_V(\boldsymbol{z},\boldsymbol{z})$ from Eq. (23), leads to

$$J = \frac{1}{2}\int_\Omega \left[\sigma_{ij}(\boldsymbol{z})(z_{i,k}V_{k,j}) + \sigma_{ij}(\boldsymbol{z})(z_{i,k}V_{k,j}) - \sigma_{ij}(\boldsymbol{z})\varepsilon_{ij}(\boldsymbol{z})\mathrm{div}\boldsymbol{V} \right] d\Omega \quad . \tag{29}$$

Defining $W = \sigma_{ij}\varepsilon_{ij}/2$ as the strain energy density and $\boldsymbol{V}(\boldsymbol{x}) = \{V_1(\boldsymbol{x}), 0\}^T$ as the velocity field, with $V_1(\boldsymbol{x})$ having a value of *unity* at the crack tip, *zero* along the boundary of the domain, and arbitrary elsewhere, the following is produced

$$J = \int_\Omega \left(\sigma_{ij}\frac{\partial z_i}{\partial x_1} - W\delta_{1j} \right) \frac{\partial V_1}{\partial x_j} \, d\Omega \,, \tag{30}$$

which is the same as the traditional domain form of the *J*-integral, with V_1 taking the place of *weight function q*. Hence, weight function *q* can be considered the virtual change in crack length, having a value of *unity* at the crack tip, *zero* along the boundary of the domain, and arbitrary elsewhere.

Now, consider two independent equilibrium states of the cracked body. Let state 1 correspond to the *actual* state for given boundary conditions, and let state 2 correspond to an *auxiliary* state, which can be either mode-I or mode-II near crack tip displacement and stress fields. Superposition of these two states leads to another equilibrium state (state *S*) for which the total potential energy $\Pi^{(S)}$ is

$$\Pi^{(S)} = \frac{1}{2}\int_{\Omega} \varepsilon_{ij}(\boldsymbol{z}^{(1)} + \boldsymbol{z}^{(2)}) D_{ijkl} \varepsilon_{kl}(\boldsymbol{z}^{(1)} + \boldsymbol{z}^{(2)}) d\Omega \; - \int_{\Gamma} \left(T_i^{(1)} + T_i^{(2)}\right)\left(z_i^{(1)} + z_i^{(2)}\right) d\Gamma \quad , \tag{31}$$

where $z_i^{(1)}$, $T_i^{(1)}$ are the components of displacement and external force vectors, respectively, of the *actual* state for given boundary conditions, and $z_i^{(2)}$, $T_i^{(2)}$ are the components of displacement and external force vectors, respectively, of the *auxiliary* state. By using the divergence theorem,

$$\begin{aligned} \int_{\Gamma} \left(T_i^{(1)}\right)\left(z_i^{(1)}\right) d\Gamma \; &= \int_{\Omega} \varepsilon_{ij}(\boldsymbol{z}^{(1)}) D_{ijkl} \varepsilon_{kl}(\boldsymbol{z}^{(1)}) d\Omega \quad , \quad \int_{\Gamma} \left(T_i^{(2)}\right)\left(z_i^{(2)}\right) d\Gamma \; = \int_{\Omega} \varepsilon_{ij}(\boldsymbol{z}^{(2)}) D_{ijkl} \varepsilon_{kl}(\boldsymbol{z}^{(2)}) d\Omega \quad , \\ \int_{\Gamma} \left(T_i^{(1)}\right)\left(z_i^{(2)}\right) d\Gamma \; &= \int_{\Omega} \varepsilon_{ij}(\boldsymbol{z}^{(1)}) D_{ijkl} \varepsilon_{kl}(\boldsymbol{z}^{(2)}) d\Omega \quad , \quad \int_{\Gamma} \left(T_i^{(2)}\right)\left(z_i^{(1)}\right) d\Gamma \; = \int_{\Omega} \varepsilon_{ij}(\boldsymbol{z}^{(2)}) D_{ijkl} \varepsilon_{kl}(\boldsymbol{z}^{(1)}) d\Omega \quad , \end{aligned} \tag{32}$$

which, when applied to the expanded form of Eq. 31 yields

$$\Pi^{(S)} = \Pi^{(1)} + \Pi^{(2)} + \Pi^{(1,2)} , \tag{33}$$

where

$$\Pi^{(1)} = -\frac{1}{2} a_{\Omega}\left(\boldsymbol{z}^{(1)}, \boldsymbol{z}^{(1)}\right), \quad \Pi^{(2)} = -\frac{1}{2} a_{\Omega}\left(\boldsymbol{z}^{(2)}, \boldsymbol{z}^{(2)}\right), \quad \Pi^{(1,2)} = -\frac{1}{2} a_{\Omega}\left(\boldsymbol{z}^{(1)}, \boldsymbol{z}^{(2)}\right) - \frac{1}{2} a_{\Omega}\left(\boldsymbol{z}^{(2)}, \boldsymbol{z}^{(1)}\right), \tag{34}$$

are various potential energies with

$$a_{\Omega}\left(\boldsymbol{z}^{(i)}, \boldsymbol{z}^{(j)}\right) = \int_{\Omega} \varepsilon_{ij}(\boldsymbol{z}^{(i)}) D_{ijkl} \varepsilon_{kl}(\boldsymbol{z}^{(j)}) d\Omega \;\; ; i, j = 1,2 \; . \tag{35}$$

Hence, the *J*-integral for the superposed state, denoted by $J^{(S)}$, can be obtained as

$$J^{(S)} \equiv -\dot{\Pi}^{(S)} = -\dot{\Pi}^{(1)} - \dot{\Pi}^{(2)} - \dot{\Pi}^{(1,2)} . \tag{36}$$

Again, if the velocity field is defined such that $\boldsymbol{V}(\boldsymbol{x}) = \boldsymbol{0}$ on the traction-loading boundary Γ and under similar considerations, $a_{\Omega}\left(\dot{\boldsymbol{z}}^{(i)}, \boldsymbol{z}^{(j)}\right) = a_{\Omega}\left(\boldsymbol{z}^{(i)}, \dot{\boldsymbol{z}}^{(j)}\right) = -a_V'\left(\boldsymbol{z}^{(i)}, \boldsymbol{z}^{(j)}\right); i, j = 1,2$, yielding

$$J^{(S)} = -\frac{1}{2} a_V'\left(\boldsymbol{z}^{(1)}, \boldsymbol{z}^{(1)}\right) - \frac{1}{2} a_V'\left(\boldsymbol{z}^{(2)}, \boldsymbol{z}^{(2)}\right) - \frac{1}{2} a_V'\left(\boldsymbol{z}^{(1)}, \boldsymbol{z}^{(2)}\right) - \frac{1}{2} a_V'\left(\boldsymbol{z}^{(2)}, \boldsymbol{z}^{(1)}\right) . \tag{37}$$

On further expansion, $J^{(S)}$ can be decomposed to

$$J^{(S)} = J^{(1)} + J^{(2)} + M^{(1,2)} , \tag{38}$$

where

$$J^{(1)} = -\dot{\Pi}^{(1)} = -\frac{1}{2} a_V'\left(\boldsymbol{z}^{(1)}, \boldsymbol{z}^{(1)}\right), \quad J^{(2)} = -\dot{\Pi}^{(2)} = -\frac{1}{2} a_V'\left(\boldsymbol{z}^{(2)}, \boldsymbol{z}^{(2)}\right), \tag{39}$$

are the *J*-integrals for states 1 and 2, respectively, noting that $a_V'\left(\boldsymbol{z}^{(1)}, \boldsymbol{z}^{(2)}\right) = a_V'\left(\boldsymbol{z}^{(2)}, \boldsymbol{z}^{(1)}\right)$,

$$M^{(1,2)} = -\dot{\Pi}^{(1,2)} = -a_V'\left(\boldsymbol{z}^{(1)}, \boldsymbol{z}^{(2)}\right) , \tag{40}$$

is the mutual potential energy release rate. From Eq. (23) it follows

$$M^{(1,2)} = \int_{\Omega} \left[\sigma_{ij}\left(\boldsymbol{z}^{(1)}\right) \frac{\partial z_i^{(2)}}{\partial x_1} + \sigma_{ij}\left(\boldsymbol{z}^{(2)}\right) \frac{\partial z_i^{(1)}}{\partial x_1} - W^{(1,2)} \delta_{1j} \right] \frac{\partial V_1}{\partial x_j} \, d\Omega , \tag{41}$$

where $W^{(1,2)} = \left[\sigma_{ij}\left(\boldsymbol{z}^{(1)}\right) \varepsilon_{ij}\left(\boldsymbol{z}^{(2)}\right) + \sigma_{ij}\left(\boldsymbol{z}^{(2)}\right) \varepsilon_{ij}\left(\boldsymbol{z}^{(1)}\right) \right] / 2$ is the mutual strain energy density.

Stress Intensity Factors

For linear-elastic solids, the $\tilde{J}$-integral also represents the energy release rate and, as a result,

$$\tilde{J} = \alpha_{11} K_I^2 + \alpha_{12} K_I K_{II} + \alpha_{22} K_{II}^2 , \tag{42}$$

where

$$\alpha_{11} = -\frac{a_{22}}{2}\,\mathrm{Im}\left(\frac{\mu_1+\mu_2}{\mu_1\mu_2}\right), \quad \alpha_{22} = \frac{a_{11}}{2}\,\mathrm{Im}\left(\mu_1+\mu_2\right), \quad \alpha_{12} = -\frac{a_{22}}{2}\,\mathrm{Im}\left(\frac{1}{\mu_1\mu_2}\right) + \frac{a_{11}}{2}\,\mathrm{Im}\left(\mu_1\mu_2\right). \tag{43}$$

Regardless of how the auxiliary fields are defined, when Eq. (42) is applied to states 1, 2, and *S*, the following is produced

$$\tilde{J}^{(1)} = \alpha_{11}K_I^{(1)2} + \alpha_{12}K_I^{(1)}K_{II}^{(1)} + \alpha_{22}K_{II}^{(1)2}, \quad \tilde{J}^{(2)} = \alpha_{11}K_I^{(2)2} + \alpha_{12}K_I^{(2)}K_{II}^{(2)} + \alpha_{22}K_{II}^{(2)2}, \tag{44}$$

and

$$\begin{aligned}
\tilde{J}^{(S)} &= \alpha_{11}\left(K_I^{(1)}+K_I^{(2)}\right)^2 + \alpha_{12}\left(K_I^{(1)}+K_I^{(2)}\right)\left(K_{II}^{(1)}+K_{II}^{(2)}\right) + \alpha_{22}\left(K_{II}^{(1)}+K_{II}^{(2)}\right)^2 \\
&= \begin{array}{l}\alpha_{11}K_I^{(1)2} + \alpha_{12}K_I^{(1)}K_{II}^{(1)} + \alpha_{22}K_{II}^{(1)2} + \alpha_{11}K_I^{(2)2} + \alpha_{12}K_I^{(2)}K_{II}^{(2)} + \alpha_{22}K_{II}^{(2)2} \\ +2\alpha_{11}K_I^{(1)}K_I^{(2)} + \alpha_{12}\left(K_I^{(1)}K_{II}^{(2)} + K_I^{(2)}K_{II}^{(1)}\right) + 2\alpha_{22}K_{II}^{(1)}K_{II}^{(2)}\end{array} \\
&= \tilde{J}^{(1)} + \tilde{J}^{(2)} + 2\alpha_{11}K_I^{(1)}K_I^{(2)} + \alpha_{12}\left(K_I^{(1)}K_{II}^{(2)} + K_I^{(2)}K_{II}^{(1)}\right) + 2\alpha_{22}K_{II}^{(1)}K_{II}^{(2)}
\end{aligned} \tag{45}$$

By comparing Eqs. (38) and (45), the following can be obtained

$$\tilde{M}^{(1,2)} = 2\alpha_{11}K_I^{(1)}K_I^{(2)} + \alpha_{12}\left(K_I^{(1)}K_{II}^{(2)} + K_I^{(2)}K_{II}^{(1)}\right) + 2\alpha_{22}K_{II}^{(1)}K_{II}^{(2)}. \tag{46}$$

If a similar procedure is followed and the intensity of the auxiliary state is judiciously chosen, then the SIFs for orthotropic materials can derived as

$$M^{(1,I)} = 2\alpha_{11}K_I^{(1)} + \alpha_{12}K_{II}^{(1)}, \quad M^{(1,II)} = \alpha_{12}K_I^{(1)} + 2\alpha_{22}K_{II}^{(1)}. \tag{47}$$

where $M^{(1,I)}$ and $M^{(1,II)}$ are the mutual potential energy release rates for modes I and II, respectively and can be evaluated using Eq. (40). Eq. (47) provide a system of linear algebraic equations that can be solved for SIFs $K_I^{(1)}$ and $K_{II}^{(1)}$ under various mixed-mode loading conditions. In general, a numerical method is required for calculating $M^{(1,I)}$ and $M^{(1,II)}$.

Compared with existing methods, the proposed method has several advantages: (1) the calculation of SIFs is simple and straightforward as it only requires multiplication of displacement vectors and stiffness sensitivity matrices; (2) since Ω_c is small and the velocity field outside Ω_c is zero, the method only requires displacement response in Ω_c, rendering it computationally efficient; (3) the accuracy of SIF estimates is not affected by a lack of smooth transition between mesh resolutions inside and outside Ω_e, as demonstrated by numerical results; and (4) the method is applicable to multiple interacting cracks even if crack tips are close to one other. Also, in contrast to existing methods, such as the J_k^*-integral method, there is no need to perform integration along the crack face of the discontinuity (e.g., in calculating J_2^*). Hence, the proposed method is also simpler and more efficient than existing methods.

NUMERICAL EXAMPLES

An orthotropic square plate of dimensions $2L = 2W = 20$ units with a central crack of length $2a = 2$ units, investigated earlier by Oztuk and Erdogan [7] is considered. Both crack-face pressure loading, and fixed grip loading (under a constant strain) were considered. Material property data as given in Oztuk and Erdogan [7] are employed for XFEM analysis. Two different values of the shear parameter $\kappa = -0.25$ and 5.0 are employed. Normalized stress intensity factors $K_I(a)\Big/\left(\sigma_0\sqrt{\pi a}\right)$ and $K_I(-a)\Big/\left(\sigma_0\sqrt{\pi a}\right)$ under uniform crack face pressure loading for $\kappa = -0.25$ by the proposed method are respectively 1.0108 and 1.0108, which match very well with reported values of 1.0 and 1.0 by Oztuk and Erdogan [7]. Similarly, $K_I(a)\Big/\left(\sigma_0\sqrt{\pi a}\right)$ and $K_I(-a)\Big/\left(\sigma_0\sqrt{\pi a}\right)$ under uniform crack face pressure loading for $\kappa = 5.0$ by the proposed method are respectively 1.0338 and 1.0338, which match very well with reported values of 1.0 and 1.0 by Oztuk and Erdogan [7].

SUMMARY AND CONCLUSIONS

This paper presents extended finite element method (X-FEM) based continuum shape sensitivity method for calculating the mixed-mode stress-intensity factors of a stationary crack in two-dimensional, linear-elastic materials with arbitrary geometry. The method involves the material derivative concept taken from continuum mechanics, the mutual potential energy release rate, and direct differentiation. The governing variational equation is differentiated prior to discretization. The discrete form of the mutual potential energy release rate is simple and easy to calculate, as it only requires multiplication of displacement vectors and stiffness sensitivity matrices. X-FEM

based numerical examples, which comprise mode-I and mixed-mode deformations, are presented to evaluate the accuracy of the fracture parameters calculated by the proposed method. Comparisons have been made between stress-intensity factors predicted by the proposed method and available reference solutions in the literature, generated either analytically or numerically using various other fracture integrals or analyses. Excellent agreement is obtained between the results of the proposed method and previously obtained solutions. Therefore, the proposed X-FEM based shape sensitivity analysis provides an attractive alternative to fracture analysis of cracks.

ACKNOWLEDGEMENT

The authors would like to acknowledge the financial support by the Board of Research in Nuclear Sciences, India (2009/36/13-BRNS/191).

REFERENCES

[1] Moës, N., Dolbow, J., and Belytschko, T., "A finite element method for crack growth without remeshing," *International Journal for Numerical Methods in Engineering*, Vol. 46, pp. 131–150, 1999.

[2] Daux, C., Moës, N., Dolbow, J., Sukumar, N., and Belytschko, T., "Arbitrary branched and intersecting cracks with the extended finite element method," *International Journal for Numerical Methods in Engineering*, Vol. 48, pp. 1741–1760, 2000.

[2] Chen, G., Rahman, S., and Y. H. Park, "Shape Sensitivity and Reliability Analyses of Linear-Elastic Cracked Structures," *International Journal of Fracture*, Vol. 112, No. 3, 2001, pp. 223-246.

[3] Chen, G., Rahman, S. and Park, Y. H., "Shape Sensitivity Analysis in Mixed-Mode Fracture Mechanics," *Computational Mechanics*, Vol. 27, No. 4, 2001, pp. 282-291.

[4] Chen, G., Rahman, S., and Y. H. Park, "Shape Sensitivity Analysis of Linear-Elastic Cracked Structures," *ASME Journal of Pressure Vessel Technology*, Vol. 124, No. 4, pp. 476-482, 2002.

[5] Rao, B. N., and Rahman, S., "A Continuum Shape Sensitivity Method for Fracture Analysis of Isotropic Functionally Graded Materials," *Computational Mechanics*, Vol. 38, No. 2, 2006, pp. 133–150.

[7] Oztuk, M., Erdogan, F., "Mode I crack problem in an inhomogeneous orthotropic medium," International Journal of Engineering Science, Vol. 35, No. 9, pp. 869–883, 1997.